C–H local modes in cyclobutene. II. Laser photoacoustic studies 10000–17000 cm− 1. Vibrational structure and C–H local mode dynamics

J. E. Baggott, D. W. Law, P. D. Lightfoot, and I. M. Mills

Citation: The Journal of Chemical Physics **85**, 5414 (1986); doi: 10.1063/1.451606
View online: http://dx.doi.org/10.1063/1.451606
View Table of Contents: http://scitation.aip.org/content/aip/journal/jcp/85/10?ver=pdfcov
Published by the AIP Publishing

C–H local modes in cyclobutene. II. Laser photoacoustic studies 10 000–17 000 cm^{-1}. Vibrational structure and C–H local mode dynamics

J. E. Baggott,[a] D. W. Law, P. D. Lightfoot, and I. M. Mills
Department of Chemistry, University of Reading, Whiteknights, P. O. Box 224, Reading, RG6 2AD, United Kingdom

(Received 9 April 1986; accepted 1 August 1986)

In part I of this study [Baggott, Clase, and Mills, Spectrochim. Acta Part A **42**, 319 (1986)] we presented FTIR spectra of gas phase cyclobutene and modeled the $v = 1$–3 stretching states of both olefinic and methylenic C–H bonds in terms of a local mode model. In this paper we present some improvements to our original model and make use of recently derived "x,K relations" to find the equivalent normal mode descriptions. The use of both the local mode and normal mode approaches to modeling the vibrational structure is described in some detail. We present evidence for Fermi resonance interactions between the methylenic C–H stretch overtones and ring C–C stretch vibrations, revealed in laser photoacoustic spectra in the $v = 4$–6 region. An approximate model vibrational Hamiltonian is proposed to explain the observed structure and is used to calculate the dynamics of the C–H stretch local mode decay resulting from interaction with lower frequency ring modes. The implications of our experimental and theoretical studies for mode-selective photochemistry are discussed briefly.

I. INTRODUCTION

High-energy stretching overtones of X–H bonds (X = C,N,O, etc.), exhibit local mode behavior in that their positions and intensities may be understood in terms of a diatomic morse oscillator formalism, in apparent contradiction to our understanding of molecular vibrations in terms of normal modes. This is particularly true of molecules containing symmetrically equivalent X–H bonds, and the work of Child and Halonen[1] and Mills and Robiette[2] has helped to reconcile this apparent contradiction, and we are now in a position to model the vibrational structure of X–H overtones starting from either pure normal mode or pure local mode basis functions provided the necessary coupling matrix elements are included in the Hamiltonian. In the local mode representation the X–H bonds are considered as independent morse oscillators with terms allowing for coupling to any symmetrically equivalent bonds included as off-diagonal elements in the Hamiltonian.[2] Such coupling is found to be most effective at low levels of vibrational excitation but becomes overwhelmed by the effects of morse anharmonicity as the excitation is increased. At very high levels of excitation the X–H stretching vibration becomes "localized."

Such localization of excitation energy led Henry[3] to suggest that energized molecules prepared by direct excitation of overtone states might not meet the requirements of rapid, statistical energy redistribution, one of the fundamental assumptions of RRKM theory.[4] Numerous experimental studies have been conducted to explore this suggestion[5–9] but, with few exceptions, the results indicate that the assumption of rapid redistribution of energy is valid. The failure to obtain unambiguous evidence for mode selectivity in reactions induced by overtone excitation leads us to abandon the notion that excitation energy may be frozen in specific bond vibrations on time scales sufficiently long to exert any noticeable effects on unimolecular reaction rates and we must, therefore, turn our attention to the mechanism by which the energy becomes redistributed. Contamination of the local mode by coupling with other molecular vibrations provides such a mechanism and so we become concerned with the *vibrational structure* of X–H bonds in such reactive systems.

In part I of this study[10] we presented FTIR spectra of gas phase cyclobutene in the range 700–9000 cm^{-1}. Cyclobutene undergoes a ring-opening reaction to form buta-1,3-diene with a low threshold ($\sim$11 300 cm^{-1}) which may be exceeded by excitation of C–H stretching overtones in the near-IR-visible region.[7,11] In part I, we established that in addition to interbond coupling between symmetrically equivalent C–H bonds, Fermi resonances couple both the olefinic C–H and ring C=C stretch vibrations, and the methylenic C–H stretch and $\alpha(CH_2)$ scissor vibrations. We modeled the vibrational structure of the C–H bonds in cyclobutene using two independent vibrational Hamiltonians, one for each type of C–H bond present, based on a local mode approach. In the present paper we have improved our model by introducing an additional parameter, achieving much better correspondence between predicted and experimental band positions for the methylenic C–H bond system. The introduction of this additional parameter is justified by reference to the corresponding normal mode model, formulated using the relations between anharmonic constants and Darling–Dennison resonance constants derived recently by Mills and Robiette[2] and Mills and Mompean.[12] The relationships between parameters of the local mode and normal mode models are described in detail.

We also present laser photoacoustic spectra of the $v = 4$–6 overtone band systems of both types of C–H bond. For the methylenic C–H bond, the observed vibrational structure is interpreted in terms of an additional Fermi resonance betweeen C–H stretch overtone states and ring C–C stretch modes. An approximate model vibrational Hamiltonian is used to interpret the experimental spectra and to pro-

[a] Author to whom correspondence should be addressed.

 0021-9606/86/225414-16$02.10

vide an estimate of the time scale within which initially localized C–H stretch excitation becomes redistributed as a consequence of the Fermi resonance. The results of these calculations are contrasted with the behavior of the olefinic C–H stretch overtones predicted by a similar analysis.

II. EXPERIMENTAL

The methods employed in the preparation and purification of cyclobutene have been described previously.[10] Absorption spectra of gas phase cyclobutene in the range 10 600–11 120 cm^{-1} were measured using pulsed laser photoacoustic techiques similar to those described by Perry *et al.*[13] Experiments were performed at the Rutherford Appleton Laboratory, Oxfordshire, where the pulsed laser system forms part of the SERC Laser Support Facility. A Lambda Physik EMG 101E XeCl exciplex laser was used to pump a FL2002 dye laser operating on the dye IR140. Output from the dye laser was passed through a nonresonant photoacoustic cell containing a Knowles BT 1759 electret microphone. A sample pressure of 506 Torr was used, measured with a Baratron 200 series pressure transducer (MKS instruments) with range 0–1000 Torr. Pulse repetition rates were typically 10 Hz. The microphone signals were amplified (EG&G 5006 fixed-gain preamplifier) and detected by a boxcar integrator consisting of an Ortec/Brookdeal model 9415 linear gate and model 9425 scan delay generator. Output signals from the boxcar were transferred to an Apple IIe microcomputer via a commercial 12-bit *A/D* converter. The resulting spectra were stored on disk for further analysis. The gain profile of the dye was determined in a separate scan by monitoring directly the output from a power meter and was used for normalization of the photoacoustic spectra.

Spectra recorded above 11 400 cm^{-1} were measured using intracavity CW dye laser photoacoustic techniques. A Coherent Inc. Innova 90-5 Ar^+ laser was used to pump a Coherent 699-01 ring dye laser operating in a standing wave configuration with the following dyes: Styryl 9M, 11 400–12 500 cm^{-1}; pyridine 1, 12 900–14 600 cm^{-1} and rhodamine 6G, 15 300–17 100 cm^{-1}. A photoacoustic cell identical to that described above was placed inside the dye laser cavity. Mechanical modulation of the excitation was achieved by chopping the Ar^+ laser pump beam, and the resulting microphone signals were phase sensitively detected by a model 5205 lock-in amplifier (EG&G). An Apple IIe microcomputer was used to tune the dye laser wavelength by incrementing the position of a three-plate birefringent filter via a micrometer controlled by a stepper motor (Oriel) and to collect the photoacoustic spectrum by interrogating the lock-in amplifier following each step. The micrometer step size was adjusted to correspond approximately to a 1 cm^{-1} increment, the resolution limit of the birefringent filter in the rhodamine 6G region. Simultaneously with each photoacoustic spectrum, the microcomputer also collected a wavelength calibration spectrum derived from optogalvanic signals from a Ne-filled hollow cathode lamp (Cathodeon) and a power spectrum for normalization. Each of these signals were processed by separate Brookdeal model PM322A phase-sensitive detectors and transferred to the microcomputer via a two-channel 12-bit *A/D* converter. Assignments of the Ne atomic transitions used in the wavelength calibration were made based on the compilation of Crosswhite,[14] and corresponding vacuum wave number values were used in three- or four-term polynomial fits to correlate wavelength with micrometer position. Such a procedure was found to be accurate to ± 0.5 cm^{-1} and peak positions in the photoacoustic spectra were found to be reproducible to within $\sim \pm 2$ cm^{-1}, despite changes of dye, optics, and alignment. The power spectrum used for normalization was obtained by monitoring the laser light reflected from one of the Brewster angle windows of the photoacoustic cell through a polarizing filter using a NRC model 815 power meter. Sample pressures varied between 50–100 Torr, measured as described above.

Infrared spectra of gas phase cyclobutene were determined using the Nicolet 7199 FTIR system using Si/quartz and Ge/KBr beamsplitters and Hg–Cd–Te and In–As detectors, as described previously.[10]

III. RESULTS AND DISCUSSION

In subsection A we deal with a general description of both the local mode/Fermi resonance and normal mode/Fermi resonance models, tailored to suit the particular requirements of the olefinic and methylenic C–H bonds in cyclobutene. We pay particular attention to the introduction of an additional parameter not included in our original model[10] and compare the results obtained with those of our previous calculations. In subsection B we present experimental spectra of the $v = 4$–6 overtone band systems and discuss the evidence for an additional Fermi resonance involving the methylenic C–H stretch and ring C–C stretch vibrations. The model Hamiltonians developed in subsections A and B are then used in subsection C to elucidate aspects of the C–H local mode dynamics.

A. The local mode/normal mode models

Following the work of Child and Halonen[1] and Mills and Robiette[2] the local mode and normal mode models are seen as equivalent descriptions which may produce identical results provided that certain relationships are established between the morse anharmonicity parameter characteristic of local modes and the usual normal mode anharmonic constants. These are the x, K relations which have been derived by Mills and Robiette[2] for molecules with two, three, and four equivalent oscillators exemplified by H_2O, NH_3, and CH_4, and by Mills and Mompean[12] for molecules with four equivalent oscillators exemplified by $H_2C{=}CH_2$ and $H_2C{=}C{=}CH_2$. In our earlier study[10] we developed the local mode model further, allowing for the introduction of stretch/bend Fermi resonance (a local mode/normal mode interaction), and used it to model the vibrational structure of both the olefinic and methylenic C–H stretch fundamentals and overtones. In the present paper, we make use of the x,K relations to derive the equivalent normal mode models, allowing us to determine normal mode anharmonic constants from our local mode parameters. The advantages of working in the normal mode basis have been discussed[12]; in particular it provides a connection between the local mode model and the theory of normal vibrations, thereby enabling us to see how the effects of interactions between stretching

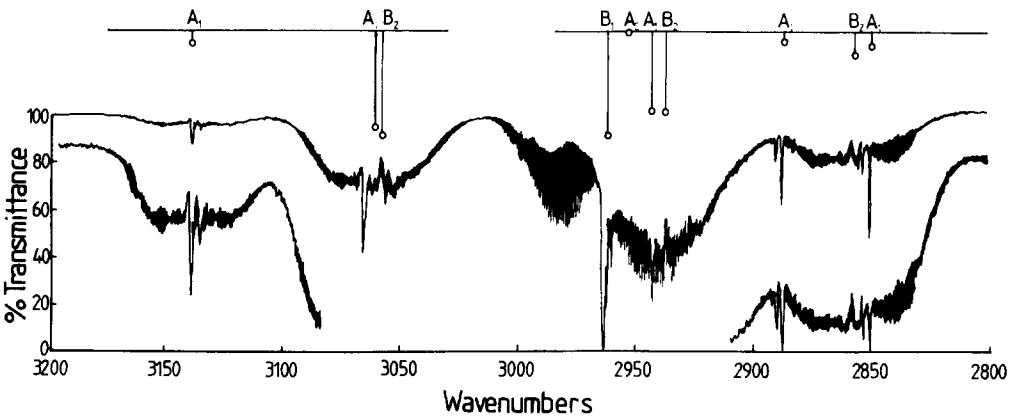

FIG. 1. FTIR spectrum in the region of the cyclobutene C–H stretch fundamentals, taken using 0.3 Torr of cyclobutene in a path length of 3.9 m. Also given are portions of a second spectrum taken using 3.0 Torr in 3.9 m. Predictions of the two model vibrational Hamiltonians are given as the sticks, with the predicted intensities represented by the lengths of the sticks.

and lower frequency vibrations should be introduced.

The FTIR spectrum given in Fig. 1 (reproduced from Ref. 10) shows that the fundamentals of both the olefinic and methylenic C–H stretching vibrations are contaminated by mixing with lower frequency modes via Fermi resonances. For the olefinic C–H bond, a somewhat novel Fermi resonance involving the ring C=C stretch ν_3 has been suggested[15,16] to account for the presence of an additional feature at 3139.4 cm^{-1}, assigned as $2\nu_3$ but *stronger* than the ν_3 fundamental. For the methylenic C–H bond a rather complex resonance arises between the symmetric stretch ν_2 and both the in-phase and out-of-phase combinations of the CH_2 scissoring vibrations ν_4 and ν_{16}, respectively. The $\nu_4 + \nu_{16}$ combination is also enhanced by Fermi resonance with the C–H stretch fundamental of B_2 symmetry ν_{15}. Although these interactions occur in a region where the normal mode description is expected to be most appropriate, we are interested to learn what, if any, effect is exerted in the region of the $v = 4$–6 C–H stretch overtones, above the threshold to unimolecular rearrangement and where the local mode model is expected to provide the best description. In the following we therefore develop both local mode and normal mode descriptions in parallel.

1. The olefinic C–H bond

The olefinic C–H bond in cyclobutene corresponds to the general case of two equivalent oscillators in Fermi reso-

TABLE I. Matrix elements (in cm^{-1}) of the effective vibrational Hamiltonian: olefinic C–H bonds.

Local mode model: $|p\rangle = |m,n;b\rangle$

$\|q\rangle$	$\langle p\|H\|q\rangle$
$\|m,n;b\rangle$	$\omega_s(m+n) + x_s[m(m+1) + n(n+1)] + \omega_b b + x_b b(b+1) + x^*_{sb}[b(m+n+1) + \frac{1}{2}(m+n)]$
$\|m-1,n+1;b\rangle$	$\lambda[m(n+1)]^{1/2}$ Interbond
$\|m+1,n-1;b\rangle$	$\lambda[n(m+1)]^{1/2}$ coupling
$\|m-1,n;b+2\rangle$	$\frac{1}{2}k_{sbb}[\frac{1}{2}m(b+1)(b+2)]^{1/2}$ Fermi
$\|m,n-1;b+2\rangle$	$\frac{1}{2}k_{sbb}[\frac{1}{2}n(b+1)(b+2)]^{1/2}$ resonance

Normal mode model[a]: $|p\rangle = |v_i,v_j;v_k\rangle$

x,K relations:

$$\omega_i = \omega_s + \lambda \quad (A_1)$$
$$\omega_j = \omega_s - \lambda \quad (B_2)$$
$$\omega_k = \omega_b$$
$$x_{ii} = x_{jj} = \tfrac{1}{4}x_{ij} = \tfrac{1}{4}K_{iijj} = \tfrac{1}{2}x_s$$
$$x_{kk} = x_b$$
$$x^*_{ik} = x_{jk} = x^*_{sb}$$
$$k_{ikk} = \sqrt{2}\,k_{sbb}$$

$\|q\rangle$	$\langle p\|H\|q\rangle$
$\|v_i,v_j;v_k\rangle$	$\omega_s(v_i+v_j) + \lambda(v_i - v_j) + \omega_b v_k + x_b v_k(v_k+1) + \frac{1}{2}x_s[v_i(v_i+1) + v_j(v_j+1) + 4\{v_i v_j + \frac{1}{2}(v_i+v_j)\}] + x^*_{sb}[v_k(v_i+v_j+1) + \frac{1}{2}(v_i+v_j)]$
$\|v_i-2,v_j+2;v_k\rangle$	$\frac{1}{2}x_s[v_i(v_i-1)(v_j+1)(v_j+2)]^{1/2}$ Darling–Dennison
$\|v_i+2,v_j-2;v_k\rangle$	$\frac{1}{2}x_s[v_j(v_j-1)(v_i+1)(v_i+2)]^{1/2}$ resonance
$\|v_i-1,v_j;v_k+2\rangle$	$\frac{1}{\sqrt{2}}k_{sbb}[\frac{1}{2}v_i(v_k+1)(v_k+2)]^{1/2}$ Fermi resonance

[a] In cyclobutene $\nu_i = \nu_1$ (CH str., A_1), $\nu_j = \nu_{14}$ (CH str., B_2), $\nu_k = \nu_3$ (C=C str., A_1).

nance with a nondegenerate "bending" vibration. We use the term bending somewhat loosely to mean a low frequency normal mode vibration; most often these are C–H bending or CH_2 scissoring vibrations, etc. In the local mode description we use unsymmetrized basis functions denoted $|m,n;b\rangle$ which are products of the $|m\rangle$ and $|n\rangle$ C–H stretch local mode states with m quanta of excitation in one bond and n quanta in the other, and of the $|b\rangle$ C=C stretch normal mode state containing b quanta of excitation. We define an overall vibrational quantum number $v = (m+n) + \frac{1}{2}b$, and v quanta of excitation leads to a total of $\frac{1}{2}(v+1)(v+2)$ basis functions which form the effective vibrational Hamiltonian. Half-odd values of v are possible and correspond to simultaneous excitation of C–H stretch and C=C stretch vibrations.

In Table I we list the diagonal and off-diagonal matrix elements appropriate for the local mode model. ω_s and x_s are the harmonic wave number and morse anharmonicity of the C–H stretch oscillators and ω_b and x_b are the harmonic wave number and anharmonicity of the normal C=C

TABLE II. Parameters of the best-fit effective vibrational Hamiltonian for the olefinic C–H bonds in cyclobutene.

Local mode model			Normal mode model	
Parameter	Value/cm^{-1} [a]	Value/cm^{-1} [b]	Parameter	Value/cm^{-1} [b]
ω_s	3179.5	3178.6	ω_i	3184.1
			ω_j	3173.1
x_s	− 59.0	− 59.0	x_{ii},x_{jj}	− 29.5
			x_{ij}	− 118.0
			K_{iijj}	− 118.0
ω_b	1578.7	1577.3	ω_k	1577.3
x_b	− 3.6	− 4.4	x_{kk}	− 4.4
x^*_{sb}		2.7	x^*_{ik},x_{jk}	2.7
λ	3.8	5.5		
k_{sbb}	27.1	30.1	k_{ikk}	42.6
rms deviation[c]	6.99	6.96		6.96

[a] Results of our earlier model (Ref. 10) in which the parameter x^*_{sb} was not included.

[b] Results of the present model.

[c] From a comparison of experimental and calculated band positions, $v = \frac{1}{2}$, 1, $\frac{3}{2}$, 2–6. In cyclobutene $\nu_i = \nu_1$, $\nu_j = \nu_{14}$, and $\nu_k = \nu_3$.

TABLE III. Comparison of experimental band positions with values predicted by the model Hamiltonian: olefinic C–H bonds.[a]

Polyad		Experiment		Model			Approx. normal
v	i	$\tilde{\nu}_i$/cm^{-1}	Γ	$\tilde{\nu}_i$/cm^{-1}	g_i	Γ	mode assignment
$\frac{1}{2}$	1	1570.5	A_1	1571.2		A_1	ν_3
1	1	3058.2	B_2	3056.4	0.500	B_2	ν_{14}
	2	3066.0	A_1	3061.2	0.460	A_1	ν_1
	3	3139.4	A_1	3139.8	0.040	A_1	$2\nu_3$
$\frac{3}{2}$	1	4620.7	?	4620.8	0.382	A_1	$\nu_1+\nu_3$
	2			4630.3	0.500	B_2	$\nu_{14}+\nu_3$
	3	4708.0	A_1	4707.5	0.118	A_1	$3\nu_3$
2	1	6015.2	A_1	6002.9	0.492	A_1	$2\nu_{14}$
	2	6019.2	B_2	6003.5	0.494	B_2	$\nu_1+\nu_{14}$
	3	6112.1	A_1	6117.1	0.001	A_1	$2\nu_1$
	4			6173.2	0.006	A_1	$\nu_1+2\nu_3$
	5	6198.2	B_2	6197.7	0.006	B_2	$\nu_{14}+2\nu_3$
	6	6274.5	?	6274.6	0.001	A_1	$4\nu_3$
3	1	8815.5	B_2	8829.3	0.496	B_2	
	2	8820.6	A_1	8829.4	0.496	A_1	
	5			9136.1	0.003	A_1	
	6			9138.6	0.004	B_2	
Total No. of states = 10							
4	1	11 531	A_1/B_2	11 537.4	0.497	B_2	
	2			11 537.4	0.497	A_1	
	5			11 971.4	0.003	A_1	
	6			11 971.6	0.003	B_2	
Total No. of states = 15							
5	1	14 123		14 127	0.498	B_2	
	2			14 127	0.498	A_1	
	5			14 686	0.002	A_1	
	6			14 686	0.002	B_2	
Total No. of states = 21							
6	1	16 601		16 599	0.498	B_2	
	2			16 599	0.498	A_1	
	5			17 282	0.002	A_1	
	6			17 282	0.002	B_2	
Total No. of states = 28							

[a] Only those states predicted to have intensities ≥ 0.001 are shown.

stretch vibration. The parameter x^*_{sb} represents the on-diagonal anharmonic constant connecting the C–H and C=C stretch states, the asterisk indicating that terms in x_{sb} containing a resonant denominator have been excluded since the Fermi resonance is treated explicitly by the introduction of suitable off-diagonal elements. (Model parameters other than x_{sb} will, of course, be affected by the omission of resonant terms.) This parameter was not introduced in our earlier treatment[10] and we justify its inclusion by reference to the corresponding normal mode description below. The diagonal elements given in Table I have been obtained by taking the ground vibrational state as the energy zero.

Two types of off-diagonal coupling are introduced. The first accounts for the interaction of the two equivalent C–H oscillators in terms of an interbond coupling parameter λ related to the potential and kinetic coupling matrix elements.[2] Interbond coupling gives rise to symmetric and antisymmetric combinations of the local mode stretch states which correlate with the A_1 and B_2 normal modes ν_1 and ν_{14}. The Fermi resonance requires the introduction of a second type of off-diagonal element, connecting basis functions of type $|m,n;b\rangle$ and $|m-1,n;b+2\rangle$, $|m,n-1;b+2\rangle$ etc. Since the two C–H stretch oscillators are identical, only one Fermi resonance coupling constant is required, and is denoted k_{sbb}. Transfer of excitation from C–H bond 1 to the C=C stretch is determined by the operator $k_{sbb}q_{s1}\,q_b^2$, where q_{s1} is the dimensionless coordinate appropriate for the local C–H stretching vibration and q_b is the dimensionless normal coordinate for the C=C stretch vibration. Similarly, transfer from bond 2 is determined by the operator $k_{sbb}q_{s2}\,q_b^2$.

The Schrödinger equation for the vth manifold expressed in matrix form:

$$\sum_s H_{rs}c_{sn} = E_n c_{rn} \tag{1}$$

is solved by diagonalization[17] of the Hamiltonian matrix **H**. We assume such matrices to be block diagonal in v, so that there are no elements connecting blocks with different values of v. The resulting eigenvalues E_n are compared with the observed band positions. In practice, nonlinear least-squares fitting[18,19] of the computed eigenvalues to the experimental band positions was performed to optimize the parameters of the model. The resulting best-fit parameters for the olefinic C–H bond system are given in Table II, where they are compared with those of our previous model.[10] In Table III and Fig. 1 the experimental band positions are compared with values computed from the best-fit parameters. The symmetries of the calculated states are obtained from an examination of the corresponding eigenvector matrix, $\mathbf{c}_n$. The relative intensity, g_i of the ith band within each polyad with vibrational quantum number v is computed as $|c_{ri}|^2$, where $|r\rangle$ corresponds to either of the pure local mode basis states $|m,0;0\rangle$ or $|0,m;0\rangle$. This procedure assumes that all the oscillator strength from the ground state is carried by the pure local mode states and that, consequently, the relative intensities of coupled states depend on the extent of mixing with the pure local modes. This model is simple and attractive but has obvious limitations. However, it appears to offer a much better approach to the problem of overtone intensities than the normal mode model.[1]

The x, K relations required to transform the local model basis into a normal mode basis are given in Table I, and are identical to those derived by Mills and Robiette for H_2O.[2] The basis functions in the normal mode model are denoted $|v_i,v_j,v_k\rangle$ and are products of the $|v_i\rangle$ and $|v_j\rangle$ C–H stretch normal modes with v_i quanta of excitation in the symmetric vibration and v_j quanta in the antisymmetric vibration and of the $|v_k\rangle$ C=C stretch normal mode containing v_k quanta of excitation. We have kept to a separate notation for the C=C stretch state for completeness, despite the fact that $|b\rangle \equiv |v_k\rangle$ when $b = v_k$. In the normal mode description the diagonal elements of the Hamiltonian matrix are given by

$$\begin{aligned}\langle v_i,v_j;v_k|H/hc|v_i,v_j;v_k\rangle &= \omega_i v_i + x_{ii}v_i(v_i+1) + \omega_j v_j + x_{jj}v_j(v_j+1) + x_{ij}\left[v_iv_j + \tfrac{1}{2}(v_i+v_j)\right] + \omega_k v_k \\ &\quad + x_{kk}v_k(v_k+1) + x^*_{ik}\left[v_iv_k + \tfrac{1}{2}(v_i+v_k)\right] + x_{jk}\left[v_jv_k + \tfrac{1}{2}(v_j+v_k)\right]\end{aligned} \tag{2}$$

and the application of the x,K relations reduces this expression to that given in Table I. The parameters x^*_{ik} and x_{jk} are the anharmonic constants for the C–H stretching and C=C stretching states. Only if these parameters are small can they be neglected, emphasizing a similar criterion for x^*_{sb} in the local mode model.

Mills[20] has summarized expressions relating generalized anharmonic constants x_{rs} to the cubic and quartic force constants. It is well known that on the application of perturbation theory, the x_{rs}'s are found to contain second-order contributions from the cubic force constants and first-order contributions from the quartic force constants of similar magnitude. Generally, for $r \neq s$,

$$x_{rs} = \frac{1}{4}\phi_{rrss} - \frac{1}{4}\sum_t (\phi_{rrt}\phi_{tss}/\omega_t) - \frac{1}{2}\sum_t \left[\phi^2_{rst}\,\omega_t\,(\omega_t^2 - \omega_r^2 - \omega_s^2)/\Delta_{rst}\right], \tag{3}$$

where

$$\Delta_{rst} = (\omega_r+\omega_s+\omega_t)(\omega_r-\omega_s-\omega_t) \times(-\omega_r+\omega_s-\omega_t)(-\omega_r-\omega_s+\omega_t)$$

and we have neglected contributions from Coriolis resonance terms. When applied to the present problem, Eq. (3) gives for x_{ik} and x_{jk}

$$x_{ik} = \frac{1}{4}\phi_{iikk} - \frac{1}{4}\frac{\phi_{iii}\phi_{ikk}}{\omega_i} - \frac{1}{2}\frac{\phi^2_{ikk}\,\omega_k}{(4\omega_k^2-\omega_i^2)}, \tag{4a}$$

$$x_{jk} = \frac{1}{4}\phi_{jjkk} - \frac{1}{4}\frac{\phi_{ijj}\phi_{ikk}}{\omega_i}, \tag{4b}$$

where we have neglected terms containing ϕ_{iik}, ϕ_{jjk}, etc. Exclusion of the resonant term in Eq. (4a) gives the expression for x^*_{ik}. In our modeling calculations we make the approximation

$$x^*_{ik} = x_{jk} = x^*_{sb} \tag{5}$$

which from Eq. (4) can be seen to depend on the similarity of the quartic force constants and of ϕ_{iii} and ϕ_{ijj}. In our previous calculations[10] we assumed these constants to be unimportant compared to the Fermi resonant terms and, indeed, this assumption appears to be valid for the olefinic C–H bond, since the introduction of x_{sb}^{*} into the model has little effect on the quality of the fit and does not change the values of the best-fit parameters significantly (see Table II). However, as will be seen below, this is not the case for the methylenic C–H bond. In the normal mode model, the magnitude of the Fermi resonance interaction is determined by the operator $k_{ikk} q_i q_k^2$, where q_i and q_k are dimensionless normal coordinates for the symmetric C–H stretch and C=C stretch vibrations, respectively. Since $q_k = q_b$ and

$$q_i = \frac{1}{\sqrt{2}} (q_{s1} + q_{s2}) \tag{6}$$

it is easily shown that $k_{ikk} = \sqrt{2} k_{sbb}$. The "Nielsen" force constant k_{ikk} is equal to $\frac{1}{2}\phi_{ikk}$. Complete interconversion between the local mode and normal mode models is now possible by applying this extended set of x,K relations. Diagonalization of the Hamiltonian matrix setup in either basis with the elements given in Table I yields identical eigenvalues. In fact, it is not necessary to set up a single matrix in the normal mode basis since we can take advantage of the symmetry of the normal modes. For example, at $v = 1$ we have a 2×2 matrix composed of the basis states $|1,0;0\rangle$ and $|0,0;2\rangle$ which have A_1 symmetry and a single unperturbed state of B_2 symmetry, $|0,1;0\rangle$.

Comparison of the experimental band positions with the predictions of the best fit model Hamiltonian in Table III shows generally good agreement. The effects of localization are very nicely illustrated by the pattern of eigenvalues produced by the model; as the vibrational excitation is increased the separation between symmetric and antisymmetric combinations of the two local C–H stretch states diminishes, and consequently, we observe predominantly single band profiles at the level of $v = 4$–6. Localization is expected to set in early for the olefinic C–H bond because of the small λ parameter, a direct consequence of the fact that the C–H bonds are separated by a C=C linkage and are therefore not likely to exhibit large potential and kinetic coupling matrix elements. The Fermi resonance interaction with the ring C=C stretch is most visible at $v = 1$ and $\frac{3}{2}$ and becomes largely unimportant at higher levels of excitation. This is due to the fact that at $v = 1$ the Fermi resonant state is *higher* in energy than the C–H stretch fundamentals; with increasing stretch excitation the gap between the basis states $|m,0;0\rangle$ and $|m-1,0;2\rangle$ in the local mode model increases due to the large anharmonicity of the local stretch states. Indeed, at $v = 4$–6 the olefinic C–H bond behaves (according to our model) as an almost "pure" local mode. We discuss the implications of such behavior in subsection C.

2. The methylenic C–H bonds

As described in part I,[10] the model used to describe the vibrational structure of the methylenic C–H stretch overtones has to be extended to account for the fact that there are now four equivalent oscillators. We denote the basis functions in the local mode model as $|m_a,n_a;m_b,n_b;b_a,b_b\rangle$ which are products of the $|m_a\rangle$ and $|n_a\rangle$ C–H stretch local mode states within one CH_2 group, $|m_b\rangle$ and $|n_b\rangle$ within the other CH_2 group and $|b_a\rangle$ and $|b_b\rangle$ which are localized $\alpha(CH_2)$ scissors vibrations belonging to each CH_2 group. The quantum numbers have the same significance as before. With mixing, the four C–H stretch local modes produce combinations which span A_1,A_2,B_1, and B_2 symmetry species and the two localized scissor vibrations produce combinations which span A_1 and B_2. The overall vibrational quantum number is defined as

$$v = (m_a + n_a + m_b + n_b) + \tfrac{1}{2}(b_a + b_b).$$

The diagonal and off-diagonal matrix elements of both the local mode and normal mode Hamiltonians are given in Table IV, together with the x,K relations used to interconvert between the two sets of basis functions. In the local mode model it becomes necessary to introduce four λ coefficients: λ_1 couples C–H bonds within a single CH_2 group, λ_2 couples bonds belonging to different CH_2 groups *cis* with respect to the molecular plane and λ_3 couple *trans* C–H bonds. λ_4 accounts for the coupling between the two localized scissor vibrations. The Fermi resonance is allowed to couple only C–H stretching and scissoring vibrations within a single CH_2 group. The remaining parameters have the same significance as before.

For the C–H stretch states the x,K relations are equivalent to those derived by Mills and Mompean[12] for ethene and for the scissoring vibrations the relations derived for H_2O are appropriate. (It may be argued that the use of x,K relations for the scissoring vibrations is inappropriate. However, the perturbation theory expressions for x_{mm}, x_{nn}, and x_{mn} exhibit these relationships for the quartic potential constants.) In the normal mode model the basis functions are denoted $|v_i,v_j,v_k,v_l;v_m,v_n\rangle$ and are products of the C–H stretch normal modes with v_i,v_j,v_k, and v_l quanta of excitation in the states of A_1,A_2,B_1, and B_2 symmetry, respectively, and of the normal scissoring vibrations containing v_m and v_n quanta in the A_1 and B_2 combinations. For cyclobutene the normal mode indices i,j,k, and l and m and n correspond to 2, 9, 15, and 21 and to 4 and 16, respectively. As for the olefinic C–H bond system, similar arguments have been applied in setting all of the x_{rs} parameters equal to each other once the Fermi resonant terms have been excluded from some of them. The usefulness of this approximation will depend on the similiarity of the quartic force constants ϕ_{iimm}, etc, and the cubic force constants $\phi_{iii},\phi_{ijj},\phi_{ikk},\phi_{ill}$, and ϕ_{jkl}. The Fermi resonances are determined by the operators $k_{imm} q_i q_m^2$, $k_{inn} q_i q_n^2$, and $k_{lmn} q_l q_m q_n$, where

$$q_i = \tfrac{1}{2}(q_{s1} + q_{s2} + q_{s3} + q_{s4}), \tag{7a}$$

$$q_l = \tfrac{1}{2}(q_{s1} + q_{s2} - q_{s3} - q_{s4}), \tag{7b}$$

$$q_m = \frac{1}{\sqrt{2}}(q_{b1} + q_{b2}), \tag{7c}$$

$$q_n = \frac{1}{\sqrt{2}}(q_{b1} - q_{b2}), \tag{7d}$$

where the q_s's are dimensionless coordinates for the localized C–H stretch vibrations and the q_b's are dimensionless

TABLE IV. Matrix elements (in cm^{-1}) of the effective vibrational Hamiltonian:methylenic C–H bonds.

Local mode model: $|p\rangle = |m_a,n_a;m_b,n_b;b_a,b_b\rangle$

$\|q\rangle$	$\langle p\|H\|q\rangle$	
$\|m_a,n_a;m_b,n_b;b_a,b_b\rangle$	$\omega_s(m_a+n_a+m_b+n_b)+x_s[m_a(m_a+1)+n_a(n_a+1)+m_b(m_b+1)+n_b(n_b+1)]+\omega_b(b_a+b_b)+x_b[b_a(b_a+1)+b_b(b_b+1)]+x_{sb}^*[b_a(m_a+n_a+m_b+n_b+2)+b_b(m_a+n_a+m_b+n_b+2)+m_a+n_a+m_b+n_b]$	
$\|m_a-1,n_a+1;m_b,n_b;b_a,b_b\rangle$	$\lambda_1[m_a(n_a+1)]^{1/2}$	interbond coupling
$\|m_a,n_a;m_b-1,n_b+1;b_a,b_b\rangle$	$\lambda_1[m_b(n_b+1)]^{1/2}$	within CH_2 group
$\|m_a-1,n_a;m_b+1,n_b;b_a,b_b\rangle$	$\lambda_2[m_a(m_b+1)]^{1/2}$	interbond coupling
$\|m_a,n_a-1;m_b,n_b+1;b_a,b_b\rangle$	$\lambda_2[n_a(n_b+1)]^{1/2}$	*cis* C–H bonds
$\|m_a-1,n_a;m_b,n_b+1;b_a,b_b\rangle$	$\lambda_3[m_a(n_b+1)]^{1/2}$	interbond coupling
$\|m_a,n_a-1;m_b+1,n_b;b_a,b_b\rangle$	$\lambda_3[n_a(m_b+1)]^{1/2}$	*trans* C–H bonds
$\|m_a,n_a;m_b,n_b;b_a-1,b_b+1\rangle$	$\lambda_4[b_a(b_b+1)]^{1/2}$	interbond coupling bending vibrations
$\|m_a-1,n_a;m_b,n_b;b_a+2,b_b\rangle$	$\frac{1}{2}k_{sbb}[\frac{1}{2}m_a(b_a+1)(b_a+2)]^{1/2}$	Fermi resonance
$\|m_a,n_a-1;m_b,n_b;b_a+2,b_b\rangle$	$\frac{1}{2}k_{sbb}[\frac{1}{2}n_a(b_a+1)(b_a+2)]^{1/2}$	within CH_2 group
$\|m_a,n_a;m_b-1,n_b;b_a,b_b+2\rangle$	$\frac{1}{2}k_{sbb}[\frac{1}{2}m_b(b_b+1)(b_b+2)]^{1/2}$	Fermi resonance
$\|m_a,n_a;m_b,n_b-1;b_a,b_b+2\rangle$	$\frac{1}{2}k_{sbb}[\frac{1}{2}n_b(b_b+1)(b_b+2)]^{1/2}$	within other CH_2 group

Normal mode model[a]: $|p\rangle = |v_i,v_j,v_k,v_l;v_m,v_n\rangle$

x,K Relations: stretches

$$\omega_i = \omega_s + \lambda_1 + \lambda_2 + \lambda_3 \ (A_1)$$
$$\omega_j = \omega_s - \lambda_1 - \lambda_2 + \lambda_3 \ (A_2)$$
$$\omega_k = \omega_s - \lambda_1 + \lambda_2 - \lambda_3 \ (B_1)$$
$$\omega_l = \omega_s + \lambda_1 - \lambda_2 - \lambda_3 \ (B_2)$$
$$x_{ii} = \tfrac{1}{4}x_{ij} = \tfrac{1}{4}K_{iijj} = \tfrac{1}{16}K_{ijkl} = \tfrac{1}{4}x_s \text{ etc.}$$

bends

$$\omega_m = \omega_b + \lambda_4 \ (A_1)$$
$$\omega_n = \omega_b - \lambda_4 \ (B_2)$$
$$x_{mm} = x_{nn} = \tfrac{1}{4}x_{mn} = \tfrac{1}{4}K_{mmnn} = \tfrac{1}{2}x_b$$
$$x_{im}^* = x_{jm} = x_{km} = x_{lm}^* = x_{in}^* = x_{jn} = x_{kn} = x_{ln}^* = x_{sb}^*$$
$$k_{imm} = k_{inn} = \tfrac{1}{2}k_{lmn} = k_{sbb}$$

$\|q\rangle$	$\langle p\|H\|q\rangle$	
$\|v_i,v_j,v_k,v_l;v_m,v_n\rangle$	$\omega_s v_s + \lambda_1(v_i+v_l-v_j-v_k)+\lambda_2(v_i+v_k-v_j-v_l)+\lambda_3(v_i+v_j-v_k-v_l)+\frac{1}{4}x_s[v_i(v_i+1)+v_j(v_j+1)+v_k(v_k+1)+v_l(v_l+1)+4\{v_i(v_j+v_k+v_l+1)+v_j(v_k+v_l+1)+v_k(v_l+1)+v_l+\frac{1}{2}v_s\}]+\omega_b v_b+\lambda_4(v_m-v_n)+\frac{1}{2}x_b[v_m(v_m+1)+v_n(v_n+1)+4\{v_m v_n+\frac{1}{2}v_b\}]+x_{sb}^*[v_m(v_s+2)+v_n(v_s+2)+v_s]$ where $v_s = v_i+v_j+v_k+v_l, v_b = v_m+v_n$	
$\|v_i-2,v_j+2,v_k,v_l;v_m,v_n\rangle$	$\frac{1}{4}x_s[v_i(v_i-1)(v_j+1)(v_j+2)]^{1/2}$	Darling–Dennison
⋮	⋮	resonance involving
$\|v_i,v_j,v_k-2,v_l+2;v_m,v_n\rangle$	$\frac{1}{4}x_s[v_k(v_k-1)(v_l+1)(v_l+2)]^{1/2}$	K_{iijj} etc.
$\|v_i-1,v_j-1,v_k+1,v_l+1;v_m,v_n\rangle$	$x_s[v_i v_j(v_k+1)(v_l+1)]^{1/2}$	Darling–Dennison
⋮	⋮	resonance involving
$\|v_i+1,v_j-1,v_k-1,v_l+1;v_m,v_n\rangle$	$x_s[v_j v_k(v_i+1)(v_l+1)]^{1/2}$	K_{ijkl}
$\|v_i,v_j,v_k,v_l;v_m-2,v_n+2\rangle$	$\frac{1}{2}x_b[v_m(v_m-1)(v_n+1)(v_n+2)]^{1/2}$	Darling–Dennison resonance for bends
$\|v_i-1,v_j,v_k,v_l;v_m+2,v_n\rangle$	$\frac{1}{2}k_{sbb}[\frac{1}{2}v_i(v_m+1)(v_m+2)]^{1/2}$	$\nu_i/2\nu_m, \nu_i/2\nu_n$
$\|v_i-1,v_j,v_k,v_l;v_m,v_n+2\rangle$	$\frac{1}{2}k_{sbb}[\frac{1}{2}v_i(v_n+1)(v_n+2)]^{1/2}$	Fermi resonance
$\|v_i,v_j,v_k,v_l-1;v_m+1,v_n+1\rangle$	$k_{sbb}[\frac{1}{2}v_l(v_m+1)(v_n+1)]^{1/2}$	$\nu_l/\nu_m+\nu_n$ Fermi resonance

[a] In cyclobutene $\nu_i = \nu_2$ (CH_2 str., A_1), $\nu_j = \nu_9$ (CH_2 str., A_2), $\nu_k = \nu_{21}$ (CH_2 str., B_1), $\nu_l = \nu_{15}$ (CH_2 str., B_2), $\nu_m = \nu_4$ [$\alpha(CH_2)$ scissor, A_1], $\nu_n = \nu_{16}$ [α (CH_2) scissor, B_2]. This list of matrix elements is intended to be illustrative rather than comprehensive.

coordinates for the localized scissor vibrations. Thus, it may be assumed that $k_{imm} = k_{inn} = \frac{1}{2}k_{lmn} = k_{sbb}$.

Use of the full local mode model, as given in Table IV, requires the handling of large matrices at high values of v which makes nonlinear least-squares optimization of the parameters very inefficient. To overcome this problem, we anticipate that the interbond coupling parameters λ_2, λ_3, and λ_4 may be rather small and we are therefore able to simplify

TABLE V. Parameters of the best-fit effective vibrational Hamiltonian for the methylenic C–H bonds in cyclobutene.

Local mode model			Normal mode model	
Parameter	Value/cm^{-1} [a]	Value/cm^{-1} [b]	Parameter	Value/cm^{-1} [b]
ω_s	3059.9	3079.0	ω_i	3065.2
			ω_j	3091.4
			ω_k	3100.0
			ω_l	3059.4
x_s	− 62.6	− 63.2	$x_{ii},x_{jj},x_{kk},x_{ll}$	− 15.8
			x_{ij},x_{ik},x_{il} x_{jk},x_{jl},x_{kl}	− 63.2
			$K_{iijj},K_{iikk},K_{iill}$ $K_{jjkk},K_{jjll},K_{kkll}$	− 63.2
			K_{ijkl}	− 252.8
ω_b	1459.7	1473.0	ω_m	1481.3
			ω_n	1464.7
x_b	− 10.7	− 3.9	x_{mm},x_{nn}	− 2.0
			x_{mn}	− 7.8
			K_{mmnn}	− 7.8
x^*_{sb}		− 12.7	$x^*_{im},x_{jm},x_{km},x^*_{lm}$ $x^*_{in},x_{jn},x_{kn},x^*_{ln}$	− 12.7
λ_1	− 19.7	− 16.7		
λ_2	3.5	3.6		
λ_3	− 0.8	− 0.7		
λ_4	7.2	8.3		
k_{sbb}	35.5	46.4	k_{immm},k_{inn}	46.4
			k_{lmn}	92.8
rms deviation[c]	12.85	5.99		5.99

[a] Results of our earlier model (Ref. 10) in which the parameter x^*_{sb} was not included.

[b] Results of the present model.

[c] From a comparison of experimental and calculated band positions, $v = \frac{1}{2}$, 1, $\frac{3}{2}$, 2, $\frac{5}{2}$, 3. In cyclobutene, $\nu_i = \nu_2$ $\nu_j = \nu_9$, $\nu_k = \nu_{21}$, $\nu_l = \nu_{15}$, $\nu_m = \nu_4$, and $\nu_n = \nu_{16}$.

the model above $v = 1$ by assuming that the two CH_2 groups become independent. The remaining parameters are transferred between the two versions of the model in the optimization. The resulting best-fit values are shown in Table V. This example demonstrates the utility of the local mode model and the x,K relations rather well, reducing the number of fitted parameters from the 38 required for an unconstrained normal mode model to just 10. In Table V we also compare the results of the present model with those of our earlier work.[10] Clearly, the parameter x^*_{sb} is now much more important, and its introduction has affected the values of all of the best-fit parameters to some extent. As might have been expected, the parameters which are most sensitive are x_b and k_{sbb}. The agreement between predicted and experimental band positions in the region of the methylenic C–H stretch fundamentals is now very good, as shown in Table VI and Fig. 1. In Table VI we also give the band positions predicted using the full model for the $v = \frac{3}{2}$, 2, $\frac{5}{2}$, and 3 overtones, although it can be seen that the model does less well at these higher energies. Perhaps surprisingly, the model recovers somewhat at $v = 3$ where the Fermi resonance becomes less important. The model breaks down rather badly at $v = 2$, where a second intense feature in the region of 5900 cm^{-1} is observed in the experimental FTIR spectra[10] in addition to the predicted intense band system in the region of 5736 cm^{-1} (Table VI). The reason for this discrepancy is not immediately obvious, but comparison with FTIR spectra of gas phase ethylene oxide[21] indicates that this second feature should indeed be assigned as belonging to the methylenic C–H stretch overtone manifold. Careful consideration of the problem in terms of normal modes leads to the assignment of the complex 5898.7 cm^{-1} band as a possible superposition of the following states:

			Predicted	Observed
$2\nu_{21}$	A_1,	type a	5915.8 cm^{-1}	5904.4 cm^{-1}
$\nu_9 + \nu_{21}$	B_2,	type b	5895.7 cm^{-1}	
$2\nu_9$	A_1,	type a	5894.2 cm^{-1}	5898.7 cm^{-1}
$\nu_2 + \nu_{21}$	B_1,	type c	5892.9 cm^{-1}	5894.0 cm^{-1}.

On closer inspection of the observed feature it is possible to identify two type a bands and a type c band (the type b bands can be difficult to identify in the presence of overlapping transitions). Thus, these seem to be in reasonable agreement although it should be recalled that these states will be heavily mixed due to the effects of Darling–Dennison and Fermi resonance. We may interpret this correspondence as a triumph for the normal mode model, since it is clearly our crude method for determining overtone intensities from the local mode picture which is failing in this case. However, by the same argument, the normal mode model would appear to be unable to provide an explanation as to why the combinations $\nu_{21} + 2\nu_{16}$, $\nu_2 + 2\nu_{16}$, and $\nu_{15} + 2\nu_{16}$ should have con-

TABLE VI. Comparison of experimental band positions with values predicted by the model Hamiltonian: methylenic C–H bonds.[a]

Polyad		Experiment		Model			Approx. normal mode
v	i	$\tilde{\nu}_i/\mathrm{cm}^{-1}$	Γ	$\tilde{\nu}_i/\mathrm{cm}^{-1}$	g_i	Γ	assignment
$\frac{1}{2}$	1	1432.4	B_2	1431.6		B_2	ν_{16}
	2	1449.4	A_1	1448.3		A_1	ν_4
1	1	2850.2	A_1	2849.1	0.031	A_1	$2\nu_{16}$
	2	2858.1	B_2	2855.5	0.051	B_2	$\nu_4+\nu_{16}$
	3	2887.5	A_1	2886.5	0.022	A_1	$2\nu_4$
	4	2937.0	B_2	2937.0	0.199	B_2	ν_{15}
	5	2942.9	A_1	2942.5	0.198	A_1	ν_2
	6	(2955)[b]	A_2	2952.4	0.250	A_2	ν_9
	7	2963.5	B_1	2960.9	0.250	B_1	ν_{21}
$\frac{3}{2}$	1	4255.1	B_2	4254.6	0.054	B_2	$3\nu_{16}$
	2	4257.3	A_1	4256.8	0.065	A_1	$\nu_4+2\nu_{16}$
	3			4285.8	0.018	B_2	$2\nu_4+\nu_{16}$
	4			4308.8	0.006	A_1	$3\nu_4$
	5	4355.2	B_2	4363.5	0.018	B_2	$\nu_2+\nu_{16}$
	6			4366.7	0.052	A_1	$\nu_{15}+\nu_{16}$
	7	4369.7	B_1	4371.4	0.125	B_1	$\nu_9+\nu_{16}$
	8			4379.9	0.125	A_2	$\nu_{21}+\nu_{16}$
	9			4388.0	0.125	A_2	$\nu_9+\nu_4$
	10			4389.1	0.160	B_2	$\nu_{15}+\nu_4$
	11	4406.5	A_1/B_1?	4394.0	0.127	A_1	$\nu_2+\nu_4$
	12			4396.5	0.125	B_1	$\nu_{21}+\nu_4$
2	1			5644.9	0.010	A_1	$4\nu_{16}$
	2			5645.3	0.011	B_2	$\nu_4+3\nu_{16}$
	4			5698.8	0.006	B_2	$3\nu_4+\nu_{16}$
	6	5737.3	B_1	5736.7	0.197	B_1	$\nu_{21}+2\nu_{16}$
	7			5736.8	0.196	A_2	$\nu_9+2\nu_{16}$
	8	5727.5	A_1	5739.5	0.184	A_1	$\nu_2+2\nu_{16}$
	9	5733	B_2	5739.6	0.184	B_2	$\nu_{15}+2\nu_{16}$
	12			5784.1	0.009	A_2	$\nu_{21}+\nu_4+\nu_{16}$
	14			5808.2	0.015	A_2	$\nu_2+\nu_9$
	15	5809.3	B_1?	5809.3	0.035	B_1	$\nu_9+\nu_{15}$
	16			5811.8	0.014	B_2	$\nu_2+\nu_{15}$
	17			5817.9	0.021	A_1	$\nu_2+2\nu_4$
	18			5825.9	0.031	A_2	$\nu_{15}+\nu_{21}$
	19	5834.0	B_1?	5830.2	0.017	B_1	$\nu_{21}+2\nu_4$
	20			5838.5	0.029	B_2	$\nu_{15}+2\nu_4$
	21	5841.9	A_1	5840.2	0.021	A_1	$2\nu_{15}$
	26	5898.7	?	5895.7	0.006	B_2	$\nu_9+\nu_{21}$
Total No. of states = 27							
$\frac{5}{2}$	1			7022.3	0.019	B_2	
	2			7022.3	0.019	A_1	
	6			7126.4	0.152	A_2	
	7	7122.0	B_1	7126.4	0.151	B_1	
	9			7142.1	0.116	B_2	
	10	7106.5/7111.5	A_1?	7142.3	0.114	A_1	
	11			7156.2	0.020	B_1	
	12			7157.2	0.019	A_2	
	13			7162.0	0.027	A_1	
	14			7163.9	0.038	B_2	
	15			7169.0	0.019	A_1	
	23			7239.7	0.033	A_2	
	24	7220.2	B_1?	7242.5	0.041	B_1	
	25			7251.0	0.039	B_2	
	26			7254.2	0.042	A_1	
	27			7263.1	0.041	A_2	
	28			7263.9	0.035	B_1	
	29			7274.6	0.027	B_2	
	30			7275.6	0.022	A_1	
Total No. of states = 42							
3	1			8383.8	0.023	A_1	
	2			8383.8	0.023	B_2	
	3	8427.0	B_1	8422.7	0.213	A_2	
	4			8422.7	0.213	B_1	
	5	8413.6	A_1	8429.7	0.190	A_1	
	6			8429.8	0.192	B_2	

TABLE VI (*continued*).

Polyad v	i	Experiment $\tilde{\nu}_i/\text{cm}^{-1}$	Experiment Γ	Model $\tilde{\nu}_i/\text{cm}^{-1}$	Model g_i	Model Γ	Approx. normal mode assignment
	7			8448.5	0.011	A_1	
	8			8452.0	0.010	B_2	
	11			8518.3	0.026	A_2	
	12			8518.5	0.027	B_1	
	14			8540.0	0.006	B_2	
	15			8540.2	0.005	A_2	
	16			8541.0	0.007	A_1	
	18			8547.8	0.008	B_2	
	19			8549.0	0.008	A_1	
	20			8559.0	0.007	B_2	
	21			8561.0	0.005	A_1	
Total No. of states = 77							

[a] Only those states predicted to have intensities > 0.005 are shown.
[b] Taken from the study of Lord and Rea, J. Am. Chem. Soc. 79, 2401 (1957).

siderable intensity compared to combinations involving ν_4, and why combinations of stretch states involving ν_2 and ν_{15} are weak. Our problem will not be resolved until we have a realistic model for the overtone intensities, but from $v = 3$ onwards it would seem that our local mode description is adequate.

B. C–H stretch overtones in the near-IR/visible region

Laser photoacoustic spectra of the $v = 4$–6 overtone band systems of both methylenic and olefinic C–H bonds are shown in survey in Figs. 2(a)–2(c). In Fig. 2(a), the $v = 4$ band of the methylenic C–H is indicated by the roman I and was determined using pulsed laser photoacoustic spectroscopy, as described in the experimental section. The relative intensities of the methylenic and olefinic $v = 4$ overtone bands, I and II, respectively, in Fig. 2(a), are difficult to quantify since two different spectroscopic techniques have been used in their determination.

The olefinic C–H stretch overtones show the anticipated local mode progression and above $v = 4$ consist largely of single bands with no apparent splitting due to coupling with other molecular vibrations. Shoulders do appear in the $v = 6$ band profile in Fig. 2(c) although it is not impossible that these minor bands belong to the methylenic C–H stretch overtone system. The experimental band positions and widths for both types of C–H bond are summarized in Table VII. The band positions of the $v = 4$–6 overtones of the olefinic C–H stretch are in accord with the predictions of the local mode/Fermi resonance Hamiltonian used to model the $v = \frac{1}{2} - 3$ band positions. The model, whose parameters are summarized in Table II, predicts that bands of A_1 and B_2 symmetry of equal intensity are to be expected for each overtone. These bands are predicted to have the same energy and therefore produce superimposed type *a* and type *b* rotational band contours. The predicted energies are: $v = 4$, 11 537 cm^{-1}; $v = 5$, 14 127 cm^{-1}; $v = 6$, 16 599 cm^{-1} which are in excellent agreement with the experimental values reported in Table VII.

The widths of the major olefinic C–H stretch overtone bands are largely independent of the vibrational quantum number v although the width of the $v = 6$ overtone band is slightly larger than those of the $v = 4$, 5 bands. Given that the widths of the rotational band contours of the $v = 1$, 2, and 3 bands are of the order of 50–60 cm^{-1} [10] we may conclude that the major contributions to the widths of the $v = 4$ and 5 bands are rotational in origin.

The methylenic C–H overtones show quite different behavior. In particular, the $v = 5$ band demonstrates the presence of another resonance not yet treated by any of our models thus far. The vibrational Hamiltonian used to model the $v = \frac{1}{2} - 3$ band system predicts that the higher overtones should collapse to single bands at each quantum level, similar to the case for the olefinic C–H overtones, indicating that the Fermi resonance with the $\alpha(CH_2)$ scissor vibrations becomes unimportant as the interacting levels move apart at higher v. For $v = 4$, two closely spaced local mode bands at 10 977 cm^{-1} (symmetry A_1 and B_2) and 10 981 cm^{-1} (symmetry B_1) are predicted. At $v = 5$ these bands collapse to a single band at 13 420 cm^{-1} as the interbond coupling parameter λ_1 is finally overwhelmed by the increasing gap between states with $m_a(m_b) = 5$, $n_a(n_b) = 0$, and $m_a(m_b) = 4$, $n_a(n_b) = 1$. At $v = 6$ the two superposed bands are predicted to be found at 15 731 cm^{-1}. The energy values for the $v = 5$, 6 overtones can be seen to be in *approximate* agreement with the experimental band centers given in Table VII, indicating that the resonance occurring at $v = 5$ does not significantly affect the overall band positions. However, a number of aspects of the $v = 5$, 6 overtones appear somewhat puzzling at first. For example, any resonance which causes the splitting observed at $v = 5$ might be expected to exert a similar effect at $v = 6$, as crude calculations readily show, yet the $v = 6$ overtone appears as a single, near-Lorentzian band. We therefore turn our attention to the investigation of this behavior.

In the study of Jasinski *et al.*[7] the shoulder to low energy of the main $v = 5$ methylenic C–H stretch overtone band was suggested to be a combination band involving four quanta of C–H stretch plus two quanta of an 1100 cm^{-1} vibration. Candidates for the 1100 cm^{-1} vibration were suggested

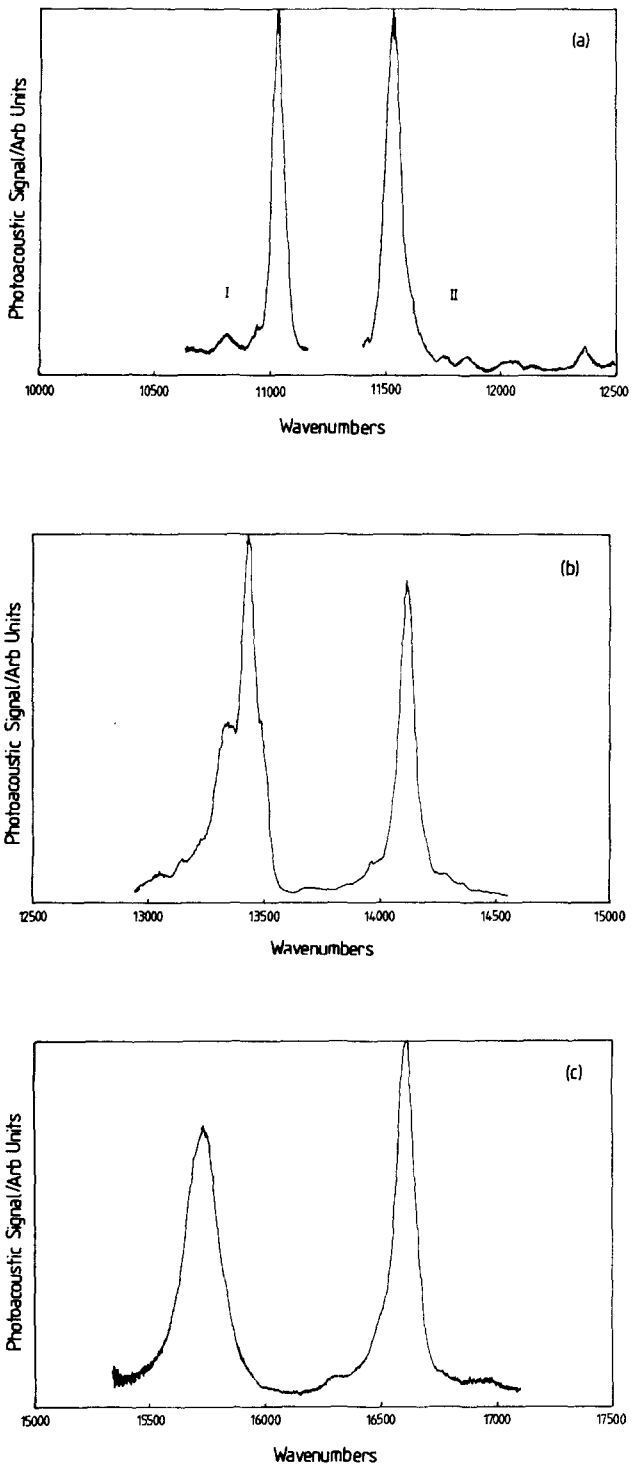

FIG. 2. (a) Laser photoacoustic spectra of the C–H stretching overtones in cyclobutene. I, Methylenic C–H $v = 4$ overtone, determined using pulsed laser techniques. II, Olefinic C–H $v = 4$ overtone, determined using intracavity CW dye laser techniques. (b) Spectra of the $v = 5$ overtone band systems of both methylenic and olefinic C–H bonds. (c) Spectra of the $v = 6$ overtone band systems of both methylenic and olefinic C–H bonds. Sample pressures were in the range 50–100 Torr except for (a) I, in which 500 Torr was used.

to be $\tau(CH_2)$ twisting (ν_{22};1075.3 cm^{-1} [10]) and ring-breathing (ring C–C stretch) modes, but an unambiguous assignment was not made. The presence of a second shoulder to high energy of the main feature (see Fig. 3) was not discussed by Jasinski *et al.*[7] but provides evidence that the candidates for what is an additional Fermi resonance are the symmetric and antisymmetric ring C–C stretch vibrations ν_6 and ν_{18}[10]:

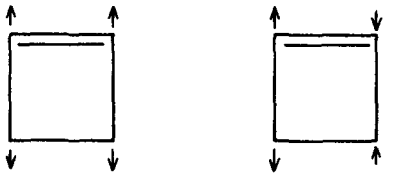

ν_6, A_1 1116.3 cm^{-1} ν_{18}, B_2 1214.3 cm^{-1}.

The high-energy shoulder indicates coupling between states with five quanta of C–H stretch and four quanta of C–H stretch plus two quanta of an approximately 1200 cm^{-1} vibration, for which ν_{18} is the only logical candidate.

We can see that the situation at $v = 5$ closely parallels the C–H stretch/$\alpha(CH_2)$ scissor Fermi resonance which we have modeled reasonably successfully and which is prominent at $v = 1$–3. However, modeling the C–H stretch/C–C ring mode Fermi resonance in a similar manner presents some difficulties. Firstly, the amount of experimental information is very limited; we have only three bands from which to extract four unknown parameters (ω_b,x_b,x_{sb}^*, and k_{sbb} appropriate for the ring C–C stretch vibrations). The parameters ω_s,x_s,λ_1,λ_2, and λ_3 are available from our earlier model (Table V) and λ_4, the interbond coupling coefficient for the two "localized" C–C stretch vibrations which gives rise to the symmetric and antisymmetric combinations, can be found from the splitting between ν_6 and ν_{18}. Secondly, the Hamiltonian matrices appropriate to the $v = 5$, 6 levels will be large (the order is 378 at $v = 5$) if the full model is used. Finally, the nuclear displacements intended to illustrate the form of the ring C–C stretch normal modes are, of course, approximate and *all* of the ring modes in the region 950–1250 cm^{-1} are likely to be heavily mixed. Furthermore, coupling between the ring modes and lower frequency modes is also likely (we shall return to this point in subsection C).

TABLE VII. Observed positions and widths of the C–H stretching overtones in cyclobutene, $v = 4$–6.

	Methylenic		Olefinic	
v	Position/ cm^{-1}	Width/ cm^{-1} [a]	Position/ cm^{-1}	Width/ cm^{-1} [a]
4	10 816	(54)	**11 531**[b]	**82**
	(10 928)*s*		11 751	(70)
	(10 949)*s*		11 845	(65)
	11 038	**65**	12 033	(95)
			12 131	(60)
			12 360	(61)
5	(13 066)*s*		(13 962)*s*	
	(13 161)*s*		**14 123**	**76**
	13 344	**155**[c]		
	13 440	**53**[c]		
	13 500	**36**[c]		
6	**15 718**	**179**	(16 303)*s*	
			(16 484)*s*	
			16 601	**101**
			(16 934)*s*	

[a] FWHM.
[b] Superposition of type *a* and *b* bands—type *b* band center given.
[c] From computer deconvolution assuming Lorentzian band shapes. Bold figures indicate main bands. *s* = shoulder. Figures in brackets are approximate.

Nevertheless, the problem is sufficiently interesting to warrant at least some form of modeling, however crude, and so we proceed as follows:

(i) From our previous experience and the results presented in Tables II and V we suspect that the anharmonicity constants appropriate for the localized ring C–C stretch should be small and we therefore assume these parameters to be negligible. ω_b may be deduced from the band positions of ν_6 and ν_{18} to be 1165.3 cm^{-1} with $\lambda_4 = -49$ cm^{-1}, the negative value indicating that the antisymmetric combination is higher in energy. The values of ω_s, x_s and of λ_1, λ_2, and λ_3 are assumed to be unchanged from our previous model (Table V). The magnitude of k_{sbb}, the force constant coupling the C–H stretch and ring C–C stretch states, is allowed to vary so as to reproduce *qualitatively*, the observed splitting pattern at $v = 5$. The diagonal and off-diagonal elements of the Hamiltonian are then calculated using the formulas given in Table IV.

(ii) The orders of the matrices are 378 at $v = 5$ and 714 at $v = 6$. While the first can be handled routinely on a large mainframe computer, the second presents problems of storage and processing time (which is proportional to the cube of the order for matrix diagonalization). These problems may be overcome by using routines designed to handle sparse matrices, but we prefer to simplify the model by truncating the basis set, since the great majority of states included in the full calculation are expected to have very little effect on the final result. There are many ways of truncating the basis set but the simplest is to terminate it after "transfer" of n quanta of excitation from the local stretch states to the C–C ring modes, where n is determined as the minimum required to produce an eigenvalue spectrum close to that obtained from the full model at $v = 5$.

(iii) We continue with our assumption that only the C–H stretch states carry oscillator strength from the ground state. The problem of determining which of the eigenstates possess A_2 symmetry, and are therefore not observed in our experimental spectra, is overcome by using the x,K relations given in Table IV to set up the problem in the normal mode description.

Given the nature of these assumptions we can expect, at best, a qualitative correspondence between predicted and experimental spectra. Nevertheless, the theoretical splitting pattern shown in Fig. 3, obtained with $k_{sbb} = 45$ cm^{-1}, shows many of the required features. In these calculations it was found necessary to include in the basis set states corresponding to the transfer of two quanta of excitation from the C–H stretch local mode, i.e., all of the intervening states between $|5,0;0,0;0,0\rangle$ and $|0,0;3;04\rangle$, making a total of 261 (rather than 378 of the full model). Diagonalization of this reduced matrix produced eigenvalues which were found to be within a few cm^{-1} of those obtained from the full model with little change in the relative intensities. We note in passing that a value of k_{sbb} of 45 cm^{-1} is entirely consistent with our earlier observations on Fermi resonances involving the methylenic C–H stretch/$\alpha(CH_2)$ scissor and olefinic C–H/ring C=C stretch vibrations (Tables III and VI). Unfortunately, we have no way of predicting the kinds of widths to be expected for the theoretical spectra shown in Fig. 3, other than to assume approximate rotational band contours, and we are therefore unable to provide a satisfactory simulation of the experimental spectrum. For the purposes of the present study it is sufficient to note that the model calculations reproduce approximately the observed spectrum; i.e., we obtain a prominent band centered at 13 429 cm^{-1} (the experimental peak value is 13 440 cm^{-1}) with shoulders at 13 345 cm^{-1} (13 344 cm^{-1}) and 13 483 cm^{-1} (13 500 cm^{-1}).

The most satisfactory aspect of our crude model emerges in the predicted splitting pattern for the $v = 6$ overtone, shown in Fig. 4. In these calculations the basis set was again truncated at states in which two quanta of stretch excitation had been transferred to the C–C ring vibration, reducing the number of states involved from 714 to 427. It is possible from Fig. 4 to see how, given suitable widths, the individual bands of the predicted spectrum might merge to produce an overall featureless, near-Lorentzian band shape. Simulations show that widths of 50 cm^{-1} for each line in the theoretical spectrum give rise to an overall band profile very similar to that observed experimentally. There are clear indications in this spectrum that we should be wary of assigning

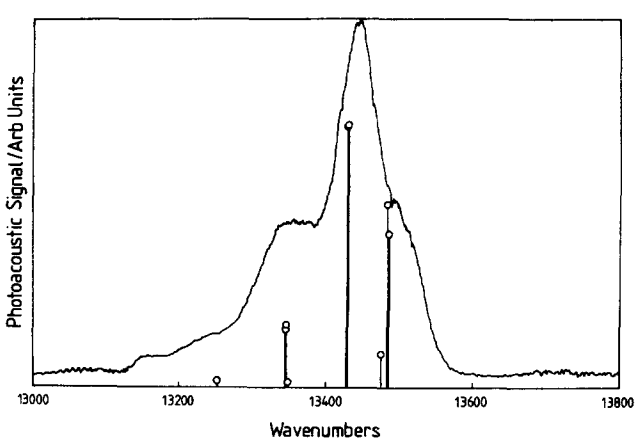

FIG. 3. Laser photoacoustic spectrum of the methylenic C–H $v = 5$ overtone. The theoretical stick spectra refer to modeling calculations based on a C–H stretch/ring C–C stretch Fermi resonance (see the text).

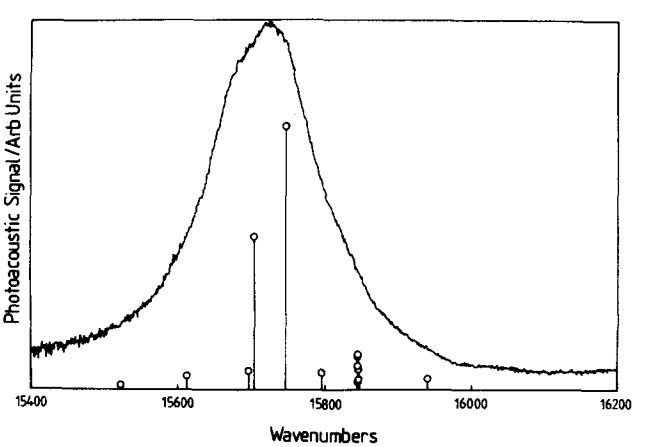

FIG. 4. Laser photoacoustic spectrum of the methylenic C–H $v = 6$ overtone. The theoretical stick spectra refer to modeling calculations based on a C–H stretch/ring C–C stretch Fermi resonance (see the text).

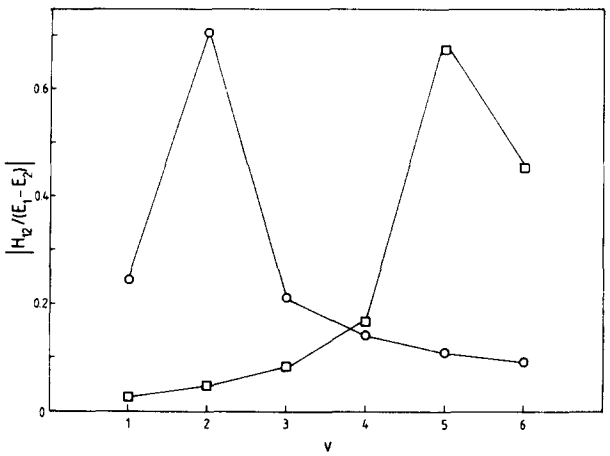

FIG. 5. Variation of the strength of Fermi resonance, measured as the ratio of the coupling matrix element/energy difference for the basis states $|m_a,0;0,0;0,0\rangle$ and $|m_a-1,0;0,0;2,0\rangle$, as a function of the overall vibrational quantum number v. (○), C–H/$\alpha(CH_2)$ scissor Fermi resonance; (□), C–H/ring C–C stretch Fermi resonance.

overtone band shapes to Lorentzians and using their widths to compute IVR rates.[22]

We feel that our crude model provides compelling evidence that the states responsible for the splitting observed in the $v=5$ overtone band profile of the methylenic C–H stretch are the ring C–C stretch modes ν_6 and ν_{18}, although these modes are likely to be heavily mixed with other ring and low frequency vibrations. Taking as a measure of the strength of the Fermi resonance interactions the ratio $|H_{12}/(E_1-E_2)|$ where H_{12} is the coupling matrix element, equal to $\frac{1}{2}k_{sbb}(m_a/2)^{1/2}$, connecting the states $|m_a,0;0,0;0,0\rangle$ and $|m_a-1,0;0,0;2,0\rangle$ and E_1-E_2 is the difference between the energies of these basis states, we can see from Fig. 5 that as the coupling between the methylenic C–H stretch local mode and the $\alpha(CH_2)$ scissor vibration becomes weaker above $v=3$, it is replaced by coupling with the ring C–C stretch modes which is strongest at $v=5$. Clearly, in separating these two interactions we are imposing some simplifying assumptions (however, treating them together in one model would require the consideration of 1892 basis states at $v=5$!), and so we would expect our Hamiltonians to be valid only in the energy region where the interaction under study is strong. Despite the many simplifications, we believe that our approach to the modeling of the vibrational structure of high-energy overtones represents a compromise which retains some useful predictive possibilities.

C. C–H local mode dynamics

Thus far we have been considering the vibrational structure of CH stretch overtone manifolds for $v=2$–6, where v is the total number of CH stretch quanta excited, and we have deduced stationary state wave functions ψ_n and energies E_n by diagonalization of the effective vibrational Hamiltonian matrix for each value of v. We have used basis functions ϕ_r which are products of pure local mode functions in the CH stretches and the overtones of the appropriate vibrations involved in the Fermi resonance; coupling terms between these basis functions arise in our model from interbond coupling terms λ and from Fermi resonance coupling terms k_{sbb}. An alternative view, which is pertinent to the suggestion that excitation of pure local mode states may lead to non-RRKM kinetic behavior, involves the elucidation of the *dynamics* of the coupled basis states.

If a molecule is promoted to an eigenstate ψ_n by interaction with a radiation field and is then undisturbed, it will remain in the state ψ_n with unchanged probability for a considerable time in our model. However, by using short-time, wide band pulsed excitation[23] we may create a superposition of a number of the eigenstates ψ_n, resulting in a time-dependent wave function of the form

$$\psi(t)=\sum_n a_n\psi_n\, e^{-iE_nt/\hbar}, \tag{8a}$$

where

$$\psi_n=\sum_r c_{rn}\phi_r\,. \tag{8b}$$

In our simple model we assume that only one of the basis functions ϕ_r is optically coupled to the ground vibrational state by a nonzero transition moment, and we denote this optically active basis function ϕ_i. Generally, for the case of two equivalent oscillators in Fermi resonance with a nondegenerate bending vibration, ϕ_i will correspond to either of the pure local mode states $|m,0;0\rangle$ or $|0,m;0\rangle$. An appropriate light pulse will put the molecule into a time-dependent wave function of the form given in Eq. (8a) where the coefficients are such that at time $t=0$,

$$\sum_n a_n\psi_n=\phi_i\,. \tag{9}$$

This defines the initial state and tells us that the coefficients a_n are actually given by the eigenvector elements c_{in} corresponding to the ith basis function under each of the eigenfunctions ψ_n, i.e.,

$$a_n=c_{in}\,. \tag{10}$$

The coefficients c_{in} are given as the eigenvectors of the matrix form of the Schrödinger equation for the vth manifold of interacting vibrational states, Eq. (1), and are obtained on diagonalization of the Hamiltonian.

We may follow the time development of the wave function Eq. (8a) from this initial state using the time development operator, $\hat{U}(t)$[24,25]

$$\Psi(t)=\hat{U}(t)\Psi(t=0)\,, \tag{11a}$$

where

$$\hat{U}(t)=e^{-i\hat{H}t/\hbar}\,. \tag{11b}$$

The density matrix in the basis functions ϕ_r is then given as a function of time by[23–26]

$$\mathbf{P}(t)=\mathbf{U}(t)\mathbf{P}(t=0)\mathbf{U}^{\dagger}(t)\,. \tag{12}$$

The rth diagonal element of $\mathbf{P}(t)$, which gives the probability of finding the system in the rth basis state at time t, may be determined from [assuming diagonal $P(t=0)$][27]

$$P_{rr}(t)=\sum_s |U_{rs}(t)|^2P_{ss}(t=0)\,. \tag{13}$$

Furthermore, if only *one* of the basis states is populated at

$t = 0$ in the manner described above, Eq. (13) reduces to

$$P_{rr}(t) = |U_{ri}(t)|^2 . \tag{14}$$

If the eigenvector elements are real (as is the case in our models) then

$$P_{rr}(t) = \sum_n c_{rn}^2 c_{in}^2 + \sum\sum_{n>m} 2c_{rm}c_{rn}c_{in}c_{im} \cos(\omega_{nm}t) , \tag{15}$$

where $\omega_{nm} = (E_n - E_m)/\hbar$. It is easily shown that

$$P_{rr}(t=0) = \left(\sum_n c_{rn}c_{in}\right)^2 \tag{16}$$

and because the eigenvector matrix **c** is orthonormal this reduces to $P_{rr}(t=0) = 1$ for $r = i$ and 0 for all other states $r \neq i$, as we should expect. Our main concern in the present study is the time development of the initial state probability

$$P_{ii}(t) = \sum_n c_{in}^4 + \sum\sum_{n>m} 2c_{im}^2 c_{in}^2 \cos(\omega_{nm}t) \tag{17}$$

and we use this expression below to estimate the time scale for decay of an initially prepared pure local mode state.

Before going on to describe the results of our calculations it is worthwhile to anticipate some of the consequences of our time-dependent view with regard to the model vibrational Hamiltonians described in subsection A. It is known from previous calculations[23,26] that Fermi resonance causes probability to flow rapidly (within ~0.1 ps) to the states $|m-1,0,2\rangle$, $|m-2,0;4\rangle$ etc., when *close to resonance*, i.e., when the energy difference between the states $|m,0;0\rangle$ and $|m-1,0;2\rangle$ is small compared to the Fermi coupling terms. Because of the relevance to observing mode selectivity, we are also interested in the behavior of the system when such resonances are very weak. Secondly, in addition to Fermi resonance, we have off-diagonal interbond coupling matrix elements which provide indirect coupling between the local mode basis states $|m,0;0\rangle$ and $|0,m;0\rangle$ (for $m = 1$ the coupling is direct). Since these states would be degenerate in the absence of coupling we anticipate complete transfer of probability from one to the other within a time τ characteristic of the splitting Δ between the eigenstates

$$\tau = \pi\hbar/\Delta . \tag{18}$$

Thus, long time scales for transfer are expected for the higher overtone states where the splitting is small. Such observations have been reported by Hutchinson *et al.*[28] in their theoretical study of coupled diatomic morse oscillators in *ABA* triatomics, based on a hindered rotor model.

In Fig. 6 we show the time-dependent probabilities for the initially prepared states $|5,0;0,0;0,0\rangle$ [Fig. 6(a)] and $|6,0;0,0;0,0\rangle$ [Fig. 6(b)] calculated using Eq. (17) and the approximate model Hamiltonian described in subsection B. Strong resonance with the ring C–C stretch vibrations results in a rapid initial state decay with approximate lifetimes of 0.12 and 0.14 ps. The dashed line in Fig. 6(a) was obtained using the full basis set (378 states) and demonstrates the validity of our simplifying assumptions. Both $|5,0;0,0;0,0\rangle$ and $|6,0;0,0;0,0\rangle$ show prominent recurrences after ~0.5–0.8 ps which, in the "real" molecule, would be

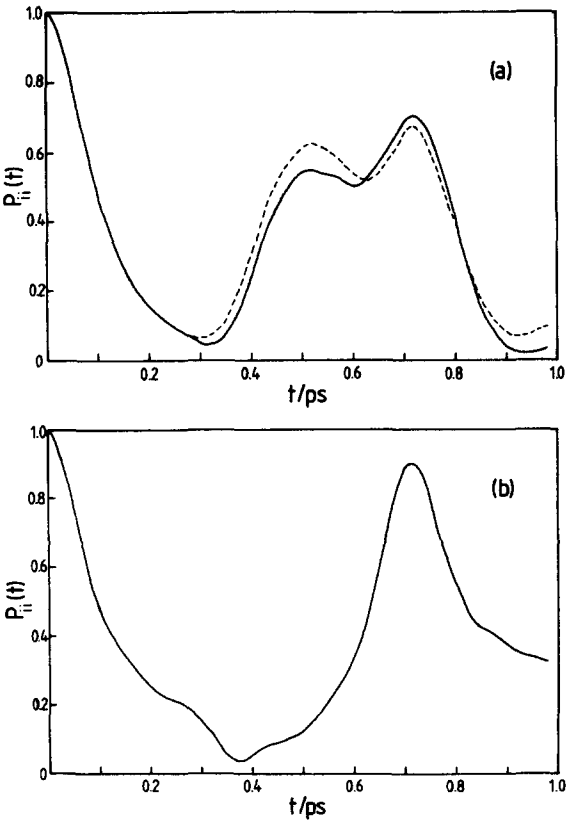

FIG. 6. Time-dependent probabilities for being in the basis states (a), $|5,0;0,0;0,0\rangle$ and (b), $|6,0;0,0;0,0\rangle$ determined from the methylenic C–H/ring C–C stretch vibrational Hamiltonian. The dashed line in (a) shows the result obtained using the full basis set at $v = 5$.

expected to be heavily damped by the effects of coupling of the ring C–C modes with other low frequency vibrations. We are primarily concerned with the time scale of the initial decay.

The results of the calculations shown in Fig. 6 represent the idealized case of an initially prepared pure local mode. The emphasis here is on the nature of state preparation, an aspect of overtone-excited reaction dynamics which has received relatively little attention. Equations (9) and (10) indicate that in order to populate a pure local mode state with unit probability we must provide ultrashort pulsed excitation of sufficiently wide bandwidth to excite *all* of the eigenstates which contain some local mode character, thereby creating a coherent superposition equivalent to Eq. (9). All experimental work performed thus far has used both pulsed and continuous narrow bandwidth excitation which is likely to produce some initial state already "contaminated" by the presence of other vibrational wave functions with significant amplitudes. Exceptions to this view will arise if the true molecular eigenfunction is best represented by a local mode function.

Figure 6 shows that any specificity attained by suitable excitation of the methylenic C–H stretch overtones in cyclobutene is rapidly lost due to strong interactions with low frequency ring modes. Since the "true" picture is likely to be an even more rapid initial state decay we can assume that energy redistribution will occur on sufficiently short time scales to ensure reaction from a statistical distribution of vibrational state populations.

Our conclusions concerning the methylenic C–H overtones provoke further questions concerning the olefinic C–H system. We have established from the vibrational spectroscopy that the $v = 4$–6 overtones of the olefinic C–H show nearly pure local mode behavior; the Fermi resonance with the ring C=C stretch becoming quickly detuned as we ascend the ladder of C–H stretch states above $v = 1$. For example, at $v = 6$ the energy difference between the basis states $|6,0;0\rangle$ and $|5,0;2\rangle$ is 688 cm^{-1} compared to a coupling matrix element of only 36.9 cm^{-1}, and we may therefore disregard this interaction as being of any consequence to the short-time dynamics of the C–H local mode. The experimental evidence from kinetic studies[7,11] indicates that excitation of the olefinic C–H stretch overtones gives isomerization rates which are readily interpreted using RRKM theory, although Hase[29] has questioned the assumption that agreement between the results of steady-state experiments and RRKM theory necessarily indicates statistical (exponential) behavior. We must recall at this stage that our model Hamiltonian is very simple and excludes many possible interactions that may be important at higher levels of excitation. We anticipate complications from a number of sources: (i) coupling might occur between the olefinic C–H stretch overtones and other lower frequency vibrations via Fermi resonance but producing only minor observable spectroscopic consequences, i.e., absence of evidence for such interactions cannot be taken as evidence of absence. There are in fact many weak unassigned bands in the high overtone spectra which may originate in Fermi resonances of this type. Candidates for such coupling would be the in-plane = C–H bending vibrations ν_5 and ν_{17} at 1185.2 and 1296.1 cm^{-1}, respectively. These vibrations have just the right fundamental frequencies to bring them into resonance at $v = 5$ and 6 (~Fig. 5). (ii) We have taken no account in our model of the possibility of Coriolis coupling. In a recent low temperature, high resolution study of the photoacoustic spectrum of the $v = 6$ C–H overtone of CH_4, Scherer *et al.*[30] discovered many rotational perturbations and suggested that in large polyatomic molecules Coriolis coupling might be as important as Fermi resonance in IVR processes, a view supported by recent classical dynamics studies.[31] Certainly, the experimental evidence for the importance of Coriolis effects on IVR within excited electronic states of large polyatomics is compelling.[32–34]

At the energy of the $|6,0;0\rangle$ basis state of the olefinic C–H the average spacing between vibrational levels is $\sim 10^{-9}$ cm^{-1}. The imposition of restrictions on which levels amongst this dense manifold are allowed to couple to the pure local mode state (however weakly) would not be expected to change the total number by more than an order of magnitude.[35] If we assume equal coupling matrix elements connecting the local mode state to all of these (equally spaced) background states we obtain a Lorentzian band profile and an exponential decay of the initial state with a lifetime proportional to the width of the Lorentzian envelope. Because of the complicated nature of the overtone band profiles determined experimentally, we cannot use the widths of the "apparently" Lorentzian band shapes to deduce initial state decay lifetimes: indeed, we believe that unresolved rotational structure accounts for a substantial fraction of the observed widths of the $v = 5$ and 6 olefinic C–H overtones. An initial *rovibrational* state decay lifetime of 1 ps would be expected to give rise to a homogeneous contribution to the widths of individual rotational lines of ~5.3 cm^{-1}, which when convoluted in a low resolution spectrum would lead to an overall broadening of the overtone band profile. From the spectra shown in Fig. 2 we can see that broadening of this magnitude is certainly a possibility. However, since we have no unambiguous method of determining the size of the homogeneous contribution to the overall widths we have no real way of determining the time scale of decay of an initially prepared local mode state, even if it were possible to create such a state experimentally.

Direct one-photon excitation of overtones in polyatomic molecules will lead to the observation of mode-specific effects only if (i) the overtone excited is negligibly coupled to other vibrational states via Fermi resonance or interbond interactions if symmetrically equivalent oscillators are involved. There should be no homogeneous broadening indicative of rapid decay into a manifold of background states (or alternatively indicative of extensive mixing with the background states). Narrow overtone band shapes are exhibited by some C–H containing polyatomic molecules, such as $CHCl_3$[36] and are common features of Si–H containing molecules such as $SiHCl_3$[37] and $SiHD_3$.[38] However, these molecules possess significantly lower densities of states at high energies compared to reactive molecules such as cyclobutene. (ii) Alternatively, if the overtone states are heavily mixed with another molecular vibration which, in terms of some unimolecular process, can be regarded as the reaction coordinate, an enhancement of the reaction rate should result.[39,40] We are currently investigating both of these above possibilities in combined spectroscopic and kinetic studies in our laboratory.

ACKNOWLEDGMENTS

JEB and IMM acknowledge support of this research by the S. E. R. C. through the award of equipment grants and a studentship (to DWL). We are grateful to John Warrington for preparing the sample of cyclobutene. We are also grateful to Graham Hogg and Dr. Martin Smith for assistance in experiments performed at the Rutherford Laboratory.

[1] M. S. Child and L. Halonen, Adv. Chem. Phys. **57**, 1 (1984).
[2] I. M. Mills and A. G. Robiette, Mol. Phys. **56**, 743 (1985).
[3] B. R. Henry, Acc. Chem. Res. **10**, 207 (1977).
[4] P. J. Robinson and K. A. Holbrook, *Unimolecular Reactions* (Wiley, New York, 1972).
[5] K. V. Reddy and M. J. Berry, Chem. Phys. Lett. **52**, 111 (1977); Faraday Discuss. Chem. Soc. **67**, 188 (1979); Chem. Phys. Lett. **66**, 223 (1979).
[6] D. W. Chandler, W. E. Farneth, and R. N. Zare, J. Chem. Phys. **77**, 4447 (1982); M.-C. Chuang, J. E. Baggott, D. W. Chandler, W. E. Farneth, and R. N. Zare, Faraday Discuss. Chem. Soc. **75**, 301 (1983).
[7] J. M. Jasinski, J. K. Frisoli, and C. B. Moore, J. Chem. Phys. **79**, 1312 (1983); Faraday Discuss. Chem. Soc. **75**, 289 (1983).
[8] T. R. Rizzo and F. F. Crim, J. Chem. Phys. **76**, 2754 (1982); F. F. Crim, Annu. Rev. Phys. Chem. **35**, 657 (1984).
[9] M.-C. Chuang and R. N. Zare, J. Chem. Phys. **82**, 4791 (1985).
[10] J. E. Baggott, H. J. Clase, and I. M. Mills, Spectrochim. Acta Part A **42**, 319 (1986).

[11]J. E. Baggott, Chem. Phys. Lett. **119**, 47 (1985).
[12]I. M. Mills and F. J. Mompean, Chem. Phys. Lett. **124**, 425 (1986).
[13]J. W. Perry, D. J. Moll, A. Kuppermann, and A. H. Zewail, J. Chem. Phys. **82**, 1195 (1985).
[14]H. M. Crosswhite, J. Res. Natl. Bur. Stand. Sect. A **79**, 17 (1975).
[15]E. M. Suzuki and J. W. Nibler, Spectrochim. Acta Part A **30**, 15 (1974).
[16]V. T. Aleksanyan and O. G. Garkusha, Izv. Akad. Nauk. Kaz. SSSR Ser. Khim, 2227 (1976).
[17]H. Rutishauser, *Handbook for Automatic Computation*, edited by J. H. Wilkinson and C. Reinsch (Springer, Berlin, 1971), Vol. II.
[18]D. W. Marquardt, J. Soc. Ind. Appl. Math. **11**, 431 (1963).
[19]P. R. Bevington, *Data Reduction and Error Analysis for the Physical Sciences* (McGraw–Hill, New York, 1969).
[20]I. M. Mills, in *Molecular Spectroscopy: Modern Research*, edited by K. N. Rao and C. W. Matthews, (Academic, New York, 1972), Vol. 1.
[21]J. E. Baggott, H. J. Clase, and I. M. Mills (unpublished results).
[22]K. V. Reddy, D. F. Heller, and M. J. Berry, J. Chem. Phys. **76**, 2814 (1982).
[23]H.-R. Dübal and M. Quack, J. Chem. Phys. **81**, 3779 (1984).
[24]A. Messiah, *Quantum Mechanics* (North-Holland, Amsterdam, 1961), Vol. 1.
[25]P. Löwdin, Adv. Quantum Chem. **8**, 323 (1967).
[26]J. E. Baggott, M.-C. Chuang, R. N. Zare, H. R. Dübal, and M. Quack, J. Chem. Phys. **82**, 1186 (1985).
[27]M. Quack, Adv. Chem. Phys. **50**, 395 (1982).
[28]J. S. Hutchinson, E. L. Sibert III, and J. T. Hynes, J. Chem. Phys. **81**, 1314 (1984).
[29]W. L. Hase, Chem. Phys. Lett. **116**, 312 (1985); J. Phys. Chem. **90**, 365 (1986).
[30]G. L. Scherer, K. K. Lehmann, and W. Klemperer, J. Chem. Phys. **81**, 5319 (1984).
[31]T. Uzer, G. A. Natanson, and J. T. Hynes, Chem. Phys. Lett. **122**, 12 (1985).
[32]D. A. Dolson, K. W. Holtzclaw, S. H. Lee, S. Munchak, C. S. Parmenter, B. M. Stones, and A. E. W. Knight, Laser Chem. **2**, 271 (1983).
[33]B. E. Forch, K. T. Chen, and E. C. Lim, Chem. Phys. Lett. **100**, 389 (1983).
[34]K. T. Chen, B. E. Forch, and E. C. Lim, *ibid.* **99**, 98 (1983); B. E. Forch, K. T. Chen, H. Saigusa, and E. C. Lim, J. Phys. Chem. **87**, 2280 (1983).
[35]M. Quack, Faraday Discuss. Chem. Soc. **71**, 359 (1981).
[36]J. S. Wong and C. B. Moore, *Proceedings of the 28th International Union of Pure and Applied Chemistry Congress*, edited by K. J. Laidler (1981), p. 353; J. E. Baggott, H. J. Clase, and I. M. Mills, J. Chem. Phys. **84**, 4193 (1986).
[37]R. A. Bernheim, F. W. Lampe, J. F. O'Keefe, and J. R. Qualey, Chem. Phys. Lett. **100**, 45 (1983).
[38]R. A. Bernheim, F. W. Lampe, J. F. O'Keefe, and J. R. Qualey, J. Mol. Spectrosc. **104**, 194 (1984).
[39]T. Uzer and J. T. Hynes, Chem. Phys. Lett. **113**, 483 (1985).
[40]T. A. Holme and J. S. Hutchinson, J. Chem. Phys. **83**, 2860 (1985).